Paramagnetic Resonance and Relaxation and Dielectric Loss in CaF_2 Crystals Containing Mn^{2+}, OH^-, and Oxygen*

FRANK MIN-TSONG LAY† AND A. W. NOLLE
Department of Physics, The University of Texas, Austin, Texas
(Received 13 June 1966; revised manuscript received 5 June 1967)

Rapid cooling from 700°C or higher of a magnetically dilute $CaF_2:Mn^{2+}$ crystal which originally gives the well-known EPR spectrum for substitutional sites produces a new cubic manganese EPR spectrum showing no contact interaction with F^- neighbors, and having the parameters $g=2.0021$, $A=-75\times10^{-4}$ cm^{-1}, $a=6.2\times10^{-4}$ cm^{-1}. Forbidden transitions in agreement with theory are found. Carrying out the preparation of the sample in a moist atmosphere increases the intensity; reheating the sample above 380°C destroys the new spectrum, but the preparation may be repeated. Oxidation of a similar original sample gives no new EPR spectrum except one due to Mn^{2+} in disoriented regions of CaO; a broad line due to concentration of Mn^{2+} in the surface region can also result from prolonged heating in the atmosphere, however. Either oxidation or hydrolysis, of samples with or without Mn^{2+}, produces dielectric loss with 1.0-eV activation energy, attributed to O^{2-} ions associated with vacancies. The paramagnetic relaxation rate (T_1^{-1}) in sec^{-1} is found to be $25T+3.8\times10^{-5}T^5$, where T is °K, for the usual $Mn^{2+}(F^-)_8$ arrangement in CaF_2, but is $19T+4.5\times10^{-4}T^{3.6}$ for the new spectrum; the change in the Raman region suggests local modes due to a complex held in the lattice by bonds of low stiffness. On the basis of all evidence, the new spectrum is provisionally ascribed to Mn^{2+} with OH^- neighbors, in cubic symmetry.

I. INTRODUCTION

THE first concern of this paper is the paramagnetic resonance and relaxation of Mn^{2+} present as an impurity in CaF_2 crystals, with and without heat treatment in atmospheres containing water vapor, hydrogen, or oxygen. It is convenient to introduce the following nomenclature: Spectrum I is the well-known EPR spectrum attributed to Mn^{2+} in substitutional sites, consisting of six clusters of superhyperfine lines.[1–3] Spectrum II, which we obtain at greatest intensity in crystals heated in the presence of water vapor, is a cubic spectrum with no superhyperfine structure. Spectrum III is a set of six sharp lines with unresolved flanking structures, which we observe after severe oxidation. Spectrum IV, which will not be considered in detail, is a broad absorption line which has occurred after prolonged heating in the atmosphere.

We describe a number of thermal treatments in specific environments, by which we have obtained spectra I, II, and III repeatedly. The spin-Hamiltonian parameters which it has been possible to measure for the various spectra are given. The longitudinal EPR relaxation rate for spectrum II is found to be markedly slower than that for spectrum I at temperatures above 15°K. Finally, further insight into oxidation and hydrolysis is obtained by observing dielectric relaxation at high temperatures in suitably treated optical-grade crystals.

It has been shown that the spectrum of a trivalent paramagnetic impurity in CaF_2 depends on the thermal history of the sample, as illustrated by the results for the rare earths.[4–7] In that case, the requirement of charge compensation affects the arrangements of imperfections (vacancies or additional impurities) near the paramagnetic ion. The present work shows that thermal treatment can produce characteristic arrangements of imperfections near a divalent impurity, where no charge compensation is involved.

II. EXPERIMENTAL WORK

A. EPR Spectra

The EPR spectra were obtained with an X-band Strandlabs spectrometer with 6 kHz field modulation, used in a 12-in. diam electromagnet with 2 in. gap. The field variation over the sample volume was less than 0.1 G. The sample was placed on the bottom of a rectangular TE_{011} cavity resonating near 9.47 GHz; the actual value with each sample was found to one part in 10^4 by an absorption wave-meter. The magnetic field was measured by NMR equipment in conjunction with a digital frequency counter. The NMR sample was approximately 1.5 cm beneath the EPR sample. The calibration and the EPR signals were recorded simultaneously on an X-Y recorder, where the X input was the sawtooth voltage from a device controlling the slow sweep of the field. The equipment calibrations were also verified by locating the resonance of polycrystalline diphenyl picryl hydrazyl (DPPH), with $g=2.0036$, a

* Supported by the National Science Foundation and the U.S. Office of Naval Research.
† Present address: Crystal Physics Laboratory, Massachusetts Institute of Technology, Cambridge, Massachusetts.
[1] J. M. Baker, W. Hayes, and D. A. Jones, Proc. Phys. Soc. (London) **73**, 942 (1959).
[2] W. Low, Phys. Rev. **105**, 793 (1957).
[3] V. M. Vinokurov and V. G. Stepanov, Fiz. Tverd. Tela **6**, 380 (1964) [English transl.: Soviet Phys.—Solid State **6**, 303 (1964)].
[4] M. Dvir and W. Low, Proc. Phys. Soc. (London) **75**, 136 (1960).
[5] W. Low, Phys. Rev. **118**, 1608 (1960).
[6] J. M. Baker, B. Bleaney, and W. Hayes, Proc. Roy. Soc. (London) **A247**, 141 (1958).
[7] W. Low and E. Friedman, J. Chem. Phys. **33**, 1275 (1960).

value with which we agreed to one part in 10^4. The sweep amplitude for this comparison was appropriate for a simultaneously recorded spectrum I, and gave an apparent derivative linewidth of 4.5 G for the DPPH signal.

B. EPR Relaxation Measurements

The low-temperature sample cavities, which were built as dual units[8] (two cavities with somewhat different frequencies, coupled to the same waveguide), were isolated from the helium bath by a vacuum-tight enclosure made of phenolic tubing coated with a suitable epoxy resin.[9] The cavity temperature was measured to about 1%, for temperatures below 50°K, by the use of a 100 Ω, $\frac{1}{10}$ W Allen Bradley resistor[10] as a sensing element. Temperatures above 50°K were obtained to within approximately 0.2°K through a copper resistance thermometer. After the liquid helium evaporated, the warming up of the probe gradually made higher temperatures available. Liquid-nitrogen temperature was reached in about 5 h. For data points so taken, the recorded temperature is the average of a warmup interval amounting usually to 2°K for the saturation method described below, or to 0.5°K for the rapid-passage method.

We followed the method described by Castner[11] in measurements of saturation of the EPR signal. The ratio of the spin-lattice relaxation times T_1 at different temperatures is inversely proportional to the ratio of the saturation powers. The relative values are adjusted to agree with the rapid-passage results to be described, in the region of overlap. No attempt is made to obtain absolute values of T_1 by the saturation method. For both methods, the size and placement of the sample were such that the microwave magnetic field variation over the sample did not exceed 5%.

Relaxation times exceeding 0.5 msec were measured by the field sweep inversion magnetization technique. The microwave auto-dyne spectrometer used for the saturation measurements was also used here, but equipped with Philco L-4153 low-noise detection diodes. The signal undergoes direct video amplification in a bandwidth of 50 kHz, and is observed on an oscilloscope. The field was first centered on the resonance value H_r and the microwave power was increased to assure saturation. Then the ac field sweep was removed. By means of a dc transistor amplifier and a pair of external coils wrapped to conform to (but not touch) the Dewar, the field was changed rapidly to approximately H_r+100 G and then, after an electronically controlled delay, to H_r-100 G. This produces a transient EPR signal, during the passage through the absorption line at about 10^5 G/sec, which is proportional to the recovered magnetization. Repetitions with various delay times yield data for a growth curve giving T_1.

The procedure of working with the apparatus temperature slowly drifting upward has the advantage that errors resulting from thermal gradients around heaters are avoided. It has the disadvantage that the electrical properties of the microwave cavity are slowly changing while the relaxation-measurement procedure is being carried out. This effect appears to be the major cause of the scatter in the present T_1 data; consequently, the error varies with the temperature and with the time required for the manipulations. An uncertainty of 15% appears to be typical, with a few larger fluctuations.

C. Dielectric Loss Measurements

Dielectric loss measurements were made by using a Boonton Model 160A Q meter in the manner described by Watkins.[12] Stainless-steel plates were used in contact with the 1×8×8 mm sample in an inert-gas-filled coaxial holder of 0.8-mm wall thickness, 20 cm long over all, which projected into an oven. In lieu of a direct measurement of sample temperature, we determined the wall temperature of the holder to ±5°C with an external thermocouple at the sample end. The end projecting from the oven was fitted with a cooling coil.

D. Preparation of Samples

1. Crystal Growing Apparatus

Those crystals which were produced in the laboratory were grown from the melt in a vacuum furnace by the Bridgman-Stockbarger method.[13,14] The 2.5-in.-diam heater, with a central hot region of reduced thickness, was machined from graphite. The heater was surrounded by three coaxial molybdenum shields to reduce radiation losses.

2. Preparation of spectrum I

For a crystal grown from a doped melt by the procedure below, no further treatment is required to obtain spectrum I (see Fig. 1). (The nomenclature of the spectra is given in the introduction.)

The growth of CaF_2 was carried out in a graphite crucible, which in most cases was 1.5 in. in diameter with a 0.020-in. wall, with a 90° point. The heater power was 3 kW. Both B. and A. reagent powder[15] and Mackay's anhydrous CaF_2 powder[16] were used as starting materials. The general procedure of Baker *et al.*[1] was followed as to the addition of PbF_2 to the powder to

[8] B. C. Thompson, G. A. Persyn, and A. W. Nolle, Rev. Sci. Instr. **34**, 943 (1963).
[9] Stycast 2850 GT, Emerson & Cuming, Inc., Canton, Massachusetts.
[10] Allen Bradley Company, Milwaukee, Wisconsin.
[11] T. G. Castner, Jr., Phys. Rev. **115**, 1506 (1959).
[12] G. D. Watkins, Phys. Rev. **113**, 91 (1959).
[13] P. W. Bridgman, Proc. Am. Acad. Arts Sci. **60**, 305 (1925).
[14] D. C. Stockbarger, J. Opt. Soc. Am. **39**, 731 (1949).
[15] Baker and Adamson brand, General Chemical Division, Allied Chemical, Morristown, New Jersey.
[16] A. D. Mackay, Inc., New York, New York.

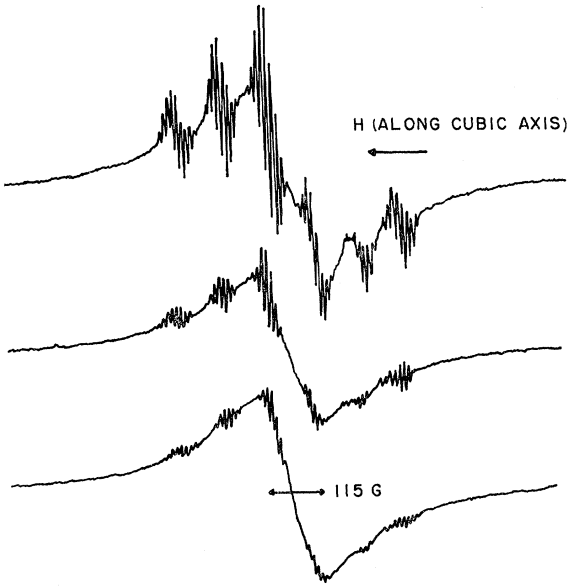

FIG. 1. Change from spectrum I to spectrum IV (broad line) with heating. The sample originally showed only the set of sharp lines, which is the well-known substitutional spectrum (spectrum I). The times of heating at 800°C in air are 2 days (top trace), 4 days, and 6 days. Heating for 10 days gives the spectrum in Fig. 3.

remove unwanted negative ions, and as to outgassing the material. At a furnace temperature of about 1150°C an influx of nitrogen was started while the vacuum pump (6 ft³/min nominal capacity) continued to operate, and was maintained thenceforth at the rate needed to maintain 800 μ pressure. The gas line contained a 200°K cold trap and an oxygen-removing section containing fine copper shavings at about 700°C. The furnace was brought to 1250°C, which was held for 2 h and then to the growth temperature of 1430°C, which was held for 2 h before the crucible was lowered at 2.75 mm/h. (Temperature readings are obtained with an optical pyrometer trained on the graphite crucible cover.) The crystal was cooled at about 100°C/h as the heating power was reduced.

Spectrum I was also found in two samples grown by the Stockbarger method by Optovac,[17] and in a diffusion-doped Harshaw[18] sample.

3. *Preparation of spectrum II*

By starting with samples giving spectrum I, we have produced spectrum II (cubic symmetry) by quenching specimens treated in suitable atmospheres, by the procedures listed below.

(a) The sample was placed in a crucible of spectroscopic-grade graphite and heated in a static argon atmosphere, contained by a quartz outer tube, to 1050°C. Upon removal from the furnace, the containing tube and contents were quenched in oil, causing the sample to reach room temperature in less than 5 min. Figure 2 shows the increasing intensity of spectrum II with various times of heating up to one week, in a particular case. Samples processed in this way have a slight yellow tint. Although this phenomenon was not investigated in detail, an absorption spectrum at room temperature was obtained for a 1-mm-thick sample with a Cary 14 spectrophotometer, which showed only a broad absorption, lacking sharp features, and too weak for accurate calibration. The sample also contains isolated nontransparent, milky regions, with a perceptible green hue. Both melt-doped and diffusion-doped starting samples have been used, with concentrations of the order of 10^{18} ions/cm³ in spectrum I. In the case shown in Fig. 2, the treatment has finally reduced the derivative-signal amplitude of spectrum I to less than 1% of the initial value. The alternative methods described below more easily yield a large ratio between the amplitudes of the two spectra, and are more rapid. (The amplitude ratio is taken here, and below, to refer to the ratio of derivative-spectrum amplitudes where

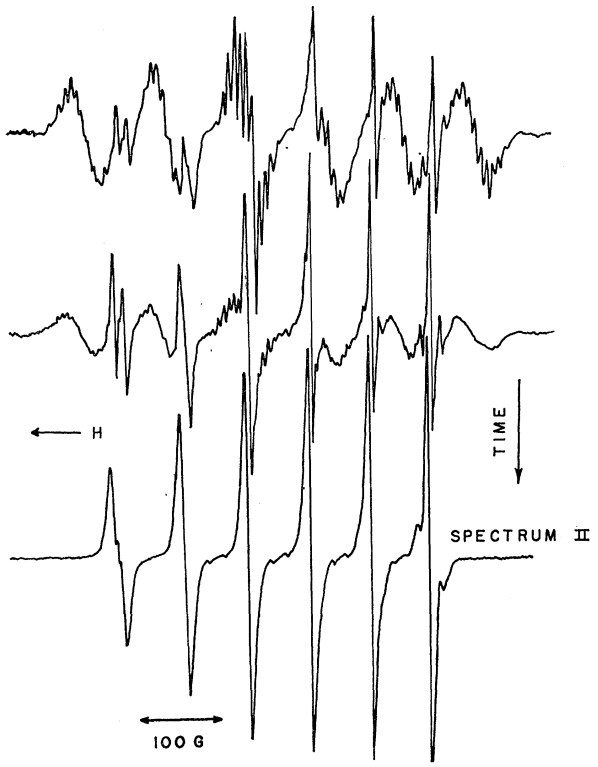

FIG. 2. Evolution of spectrum II in sample originally showing only spectrum I. Room-temperature spectra after 2 days (top trace), 4 days, and 7 days at 1050°C in argon (the conversion is more rapid with added water vapor). *H* is in the (111) plane, where the cubic structure of spectrum II collapses; the orientation is not further controlled for these runs.

[17] Optovac Inc., North Brookfield, Massachusetts.
[18] The Harshaw Chemical Company, Cleveland, Ohio.

two spectra are recorded with a single field modulation value, small compared to the linewidths in both spectra.)

(b) A treatment similar to (a) was carried out in a hydrogen atmosphere. After two days, the amplitude ratio in favor of spectrum II was at least 100. The sample appeared clear to visual inspection.

(c) A treatment similar to (a) was carried out in an ambient gas of hydrogen plus water vapor at a partial pressure of approximately 50 mm Hg. The total pressure was 1 atm, as in cases (a) and (b). Conversion to spectrum II, with an amplitude ratio of 100 or more, occurred within 4 h.

The spectra indicate that most of the manganese is retained in the short treatment (c). No careful study was made of the loss in the longer treatments, but the experience with very long treatments in oxidizing atmospheres, described in the next section, suggests that much less than half of the manganese is retained in cases (a) and (b).

4. Preparation of spectra III and IV

Prolonged heating in air of a sample which originally gives spectrum I leads to spectrum III (six sharp lines predominant). Spectrum IV, a single very broad line, has been observed [case (a) below] before spectrum III develops. Two procedures were tried, as follows:

(a) The sample was placed on a fire brick in an oven at 800°C, but removed from time to time for observation of the EPR spectrum. Figure 1 shows the spectrum at the end of the second, fourth, and sixth days. The sharp lines belong to spectrum I, which is becoming weaker with continued heating, while the broad line is spectrum IV. At the end of ten days, Spectrum III, shown in Fig. 3, is easily observable. That severe loss of manganese occurs in this process is indicated by the fact that only the surface regions of the crystal give any observable spectrum when spectrum III is finally obtained, together with the occurrence of an amorphous deposit, giving a broad EPR signal, on the surface supporting the crystal. No attempt was made to identify the deposit more completely.

(b) The sample was heated as in (a), but at 1000°C. After 24 h spectrum III was large compared to other EPR spectra from the sample. The resulting sample crumbles easily. This spectrum is found in material from the bulk or from the surface of the original block.

When the sample is kept at room temperature, in air of moderate humidity, the amplitude of spectrum III diminishes at roughly 10% per day.

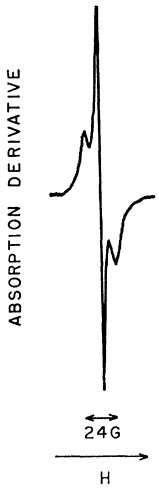

FIG. 3. High-field member of the set of six lines comprising spectrum III, which has nearly the same A as CaO:Mn^{2+}. Separation of the outer peaks, 24 G. Room temperature; there is no angular dependence.

III. EPR SPECTRA

A. Spectrum I

To verify that spectrum I is the one previously reported in the literature,[1-3] we recorded and analyzed the spectrum at X band. The spin Hamiltonian for Mn^{2+} in a cubic crystalline field is[2]

$$\mathcal{H}=g\beta\mathbf{H}\cdot\mathbf{S}+(\tfrac{1}{6})a[S_x^4+S_y^4+S_z^4-\\ -(\tfrac{1}{5})S(S+1)(3S^2-1)]+A\mathbf{S}\cdot\mathbf{I}, \quad (1)$$

where β is the Bohr magneton, and the conventional g value is used. Superhyperfine interactions with neighboring nuclei must be added as required. The allowed transitions given by (1) for the frequency ν occur at field values H given by

$$M=\pm\tfrac{5}{2}\leftrightarrow\pm\tfrac{3}{2}:$$

$$g\beta H=g\beta H_0\mp 2pa-Am-(A^2/2g\beta H_0)(35/4-m^2\pm 4m),$$

$$M=\pm\tfrac{3}{2}\leftrightarrow\pm\tfrac{1}{2}:$$

$$g\beta H=g\beta H_0\pm\tfrac{5}{2}pa-Am-(A^2/2g\beta H_0)(35/4-m^2\pm 2m),$$

$$M=\tfrac{1}{2}\leftrightarrow-\tfrac{1}{2}:$$

$$g\beta H=g\beta H_0-Am-(A^2/2g\beta H_0)(35/4-m^2), \quad (2)$$

where H_0 denotes $h\nu/g\beta$, $p=1-5\Phi$, $\Phi=l_h^2m_h^2+m_h^2n_h^2+n_h^2l_h^2$, and l_h, m_h, n_h are the direction cosines of the magnetic field direction referred to the cubic axes. Since it happens that the cubic splitting a is negligible when Mn^{2+} is substituted for Ca^{2+}, (2) reduces in the present case to six lines corresponding to values $-\frac{5}{2}$ through $\frac{5}{2}$ for m, the manganese nuclear magnetic quantum number. (Note that no terms in (2) will be neglected in connection with spectrum II, however.) The experimental spectrum (sharp lines in Fig. 1) also contains superhyperfine splitting caused by the F^- neighbors characterized by dipolar and contact interactions of respective magnitudes A_p and A_s, as described by Tink-

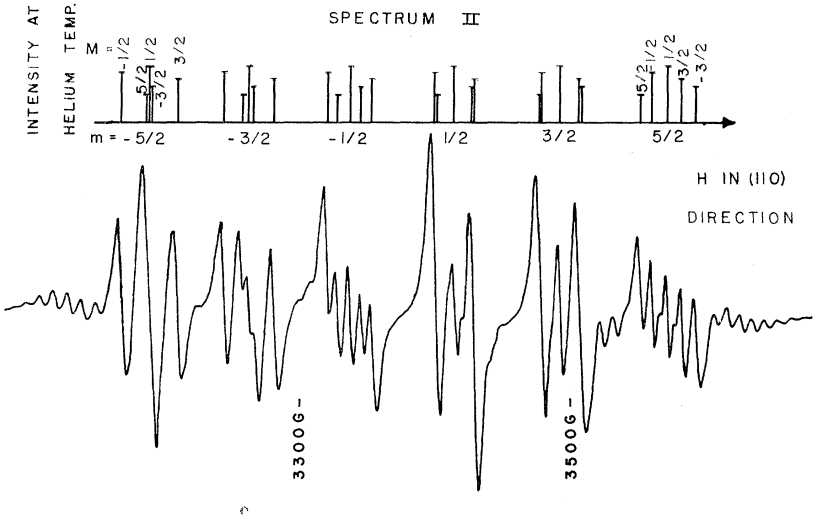

FIG. 4. Spectrum II at room temperature, 100 direction; also identification of fine-structure components, and intensity scheme predicted for $a>0$, $A<0$, in agreement with low-temperature results. A residue of spectrum I appears at the ends of the trace.

ham.[19] We found for spectrum I the room-temperature values $g=2.0015\pm0.0003$, $|A|=100\pm1$ G, $A_s=10\pm1$ G, in agreement with room-temperature published results,[3] confirming the identification (we use 1 G$=0.9375\times10^{-4}$ cm^{-1}).

B. Spectrum II

Spectrum II consists of six groups of pentads as shown in Fig. 4. There is no superhyperfine structure even at 4°K. The absence of angular variation of the spectrum with **H** in the (111) plane, and the nature of the variation observed in (100) and (110) planes, are consistent with a cubic ligand field. Figure 5 shows the agreement between line position measured in the (110) plane and calculations from Eqs. (2), which are plotted versus angle. The spin-Hamiltonian parameters found by fitting the room-temperature line positions for the [001] and [110] directions with (2) are $g=2.0021\pm0.0003$, $A=-(75\pm1)\times10^{-4}$ cm^{-1}, and $a=+(6.2\pm0.5)\times10^{-4}$ cm^{-1}. The signs are obtained by observing the spectrum at 4°K, where the intensity scheme is as sketched in Fig. 4. We further verified that additional line pairs in off-axis directions are forbidden transitions[20] $\Delta M=\pm1$ and $\Delta m=\pm1$, and are explained by available formulas[21] with the above constants.

The absence of superhyperfine structure suggests that other negative ions have replaced the normal F^- nearest neighbors of the paramagnetic ion. It was therefore of interest to observe the spectrum at elevated temperatures in a cavity and oven operable to 700°C, in order to detect modification of the spectrum by diffusion. When a sample showing spectra I and II is heated in hydrogen, spectrum II disappears at 380°C with increasing temperature, leaving spectrum I. The superhyperfine structure of spectrum I is wiped out by diffusion at 550°C. Rapid cooling from 700°C, such that the sample is cooled below 380°C within 10 min, causes spectrum II to reappear as the prominent feature. Slow cooling, requiring several hours to pass from 700°C to room temperature, gives a mixture of spectrum I and spectrum II, with I predominating. When the sample was held at 700°C for about 30 min, in vacuum instead of in the hydrogen atmosphere, rapid cooling produced spectrum II at no greater intensity than spectrum I, suggesting that the supply of negative impurity ions was reduced.

Several samples prepared to give spectrum II at high intensity (more than 10^{18} sites per cm^3) showed two weak, sharp infrared-absorption bands in spectrophotometer traces obtained at room temperature. The absorption is only 1 or 2% for a 1-mm-thick sample, and occurs near 3600 cm^{-1}. This corresponds closely to

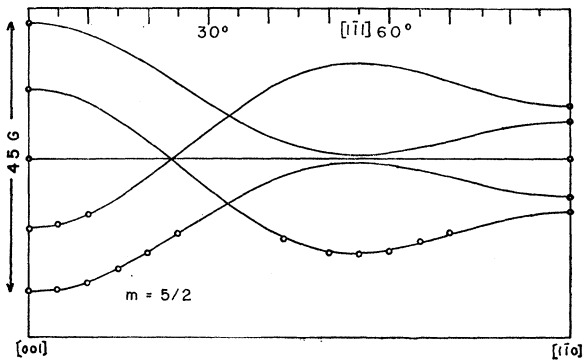

FIG. 5. Angular dependence of a single pentad hyperfine group ($m=\frac{5}{2}$) in spectrum II, in the (110) plane, shown by representative experimental points, with curves computed from Eqs. (2). In evaluation of the spin-Hamiltonian parameters, the over-all separation of the six pentads and the average separation of $M=\frac{5}{2}$ and $M=-\frac{3}{2}$ lines at 0° are used.

[19] M. Tinkham, Proc. Roy. Soc. (London) **A236,** 535 (1956).
[20] J. E. Drumheller, Helv. Phys. Acta **37,** 689 (1964).
[21] J. E. Drumheller and R. S. Rubins. Phys. Rev. **133A,** 1099 (1964).

absorption curves shown by Bontinck[22] in a study of the hydrolysis of CaF_2, and more completely explained by Wichersheim and Hanking.[23] They identified the band at 3580 cm^{-1} as the stretching vibration of hydroxyl ions substituting for fluorine, and the band at 3650 cm^{-1} as the infrared-active stretching fundamental of $Ca(OH)_2$ occurring in or on the CaF_2 crystal. None of these authors has obtained a connection between the OH^- concentration and the absorption coefficient.

There have been many reports[24] concerning the optical properties of alkali halides containing hydroxyl ions. Absorption bands at 190, 204, and 214 mμ are associated with hydroxyl impurities in NaCl, KCl, and KBr, respectively. We therefore examined spectrum-II samples also in the ultraviolet and visible ranges, but detected only broad bands near 225 and 290 mμ. These were not consistently obtained.

C. Spectra III and IV

Spectra III and IV are obtained by exposing the sample to oxygen at high temperature. The prominent feature of spectrum III is a set of six sharp lines whose separations lie between 80 and 90 G. With suitable resolution, the lines are found to have flanking structures, which are most pronounced for the low- and high-field lines, as illustrated by the tracing of the high-field line in Fig. 3. The spectrum shows no angular variation and does not change when the sample is powdered; hence, there are no well-defined axial directions. A consistent explanation is obtained by identifying the six sharp lines as the $M=\frac{1}{2}$ transitions, which have no angular dependence, in a cubic spectrum, and by identifying the flanking structures as the space average of the other four transitions of the fine structure. With random axial directions, it is impossible for any resolved superhyperfine structure to appear even if A_s is nonzero. The small width of the sharp central lines, about 2 G, shows that A_s, if not zero, is much less than 10% of the value found for spectrum I, so that it is extremely doubtful that any of the Mn^{2+} ions contributing to spectrum III have F^- neighbors. The spin-Hamiltonian parameters that can be evaluated from (2) are $g=2.0019\pm0.0003$ and $|A|=86.1\pm1$ G. The A value agrees with the results 86.2 to 86.8 G reported for Mn^{2+} in CaO,[25,26] although the g value is somewhat higher than the result 2.0010 for CaO. The spin Hamiltonian for Mn^{2+} in CaO also includes a cubic field, with $a=6.4$ G. Because we are dealing in effect with a powder sample, a test for an a of this size cannot be made accurately at X band, on account of the second-order effects due to A. For example, the term involving A^2/H_0 contributes 22 G to the separation of the $M=\frac{5}{2}\leftrightarrow\frac{3}{2}$ and $M=-\frac{3}{2}\leftrightarrow-\frac{5}{2}$ transitions, whereas the broad outer peaks in the line shown in Fig. 3 are separated by only 24 G.

Since spectrum III (a) has been found only in surface regions or in samples developing a network of cracks, (b) has not been produced with well-defined crystal axes, (c) has parameters approximating those for $CaO:Mn^{2+}$, and (d) has no fluorine superhyperfine structure, we attribute it to a configuration approximating the crystal structure of MnO, which is not stable as a complex in the bulk of the CaF_2 crystal. The real importance of spectrum III, for present purposes, is that it is the only magnetically dilute spectrum that arises from exposure of $CaF_2:Mn^{2+}$ to oxygen at high temperature. Hence spectrum II, which is produced by hydrolysis, is not attributable to a complex involving oxygen ions produced by the breakdown of H_2O. At no time has spectrum II been found even at small amplitude, in the course of producing spectrum III.

Spectrum IV, which is reported for completeness, has not been stydied extensively. It is assumed to be a high-concentration form of spectrum I, occurring when Mn_2^+ diffuses to surface regions in prolonged heating. The g value is not measurably different from 2.00. The line shape is attributed to dipolar and exchange interactions between Mn^{2+} ions. The derivative width is 115 G.

IV. SPIN-LATTICE RELAXATION

The considerable difference in the spin Hamiltonians for spectra I and II suggests that the spin-lattice relaxation times may also differ appreciably. We have therefore made an initial comparison of T_1 results for the two spectra by the experimental methods described above, examining only the transitions with $m=+\frac{5}{2}$. Because these transitions come at the end of the spectrum, they are convenient for fast-passage measurements. Only the [100] direction for H was used. In the case of spectrum II, which has the fine structure fully resolved in this direction, the results by the saturation method are for the central ($M=\pm\frac{1}{2}$) transitions, but rapid passage scans the entire pentad.

We shall fit the data for the reciprocal of the relaxation time in each case with a two-term polynomial, $aT+bT^n$, which is expected on theoretical grounds to be a useful approximation for temperatures below $\Theta_D/2$, where the Debye temperature Θ_D is 510°K for CaF_2. The terms represent, respectively, the direct and the Raman processes. A theoretical basis for using $n=5$ for the Raman process has been given by Orbach and Blume,[27] and involves consideration of a multilevel

[22] W. Bontick, Physica **24**, 650 (1958).
[23] K. A. Wichersheim and B. M. Hanking, Physica **25**, 569 (1959).
[24] J. Rolfe, Phys. Rev. Letters **1**, 56 (1958); H. W. Etzel and D. A. Patterson, Phys. Rev. **112**, 1112 (1958); R. W. Warren, Rev. Sci. Instr. **36**, 731 (1965).
[25] A. J. Shuskus, Phys. Rev. **127**, 1529 (1962).
[26] W. Low and R. S. Rubins, in *Proceedings of the First International Conference on Paramagnetic Resonance* (Academic Press Inc., New York, 1963) Vol. 1, p. 79.
[27] R. Orbach and M. Blume, Phys. Rev Letters **8**, 478 (1962).

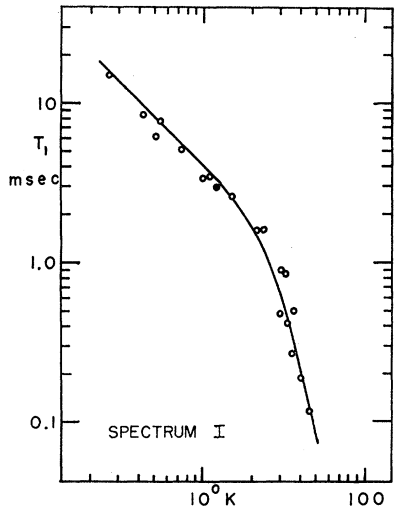

FIG. 6. Measured spin-lattice relaxation time versus temperature for spectrum I, with curve plotted from Eq. (3).

ground state ($^6S_{5/2}$ multiplet in the present case) with splitting small compared to the thermal energy kT. It has been found[28] that $n=5$ is in fact satisfactory for data on substitutional Mn^{2+} in SrF_2 and BaF_2, isomorphous to CaF_2. Accordingly, we analyze the spectrum-I relaxation data in this way with the result

$$T_1^{-1}=25T+3.8\times10^{-5}T^5 \text{ sec}^{-1}. \quad (3)$$

The T_1 curve corresponding to (3) is shown with the experimental points in Fig. 6. The Mn^{2+} concentration is estimated from the EPR absorption intensity as several times 10^{18} cm^{-3}. The result (3) was made available for a comparison,[28] which showed that the relaxation matrix elements for Mn^{2+} in the series CaF_2–SrF_2–BaF_2 increase in this order. (This phenomenon is discussed in the Ref. 28.) That this order can be obtained shows that the present relaxation rates cannot have been greatly enhanced by concentration effects, as compared to the SrF_2 and BaF_2 samples in the comparison, which had total manganese concentrations somewhat below 10^{18} cm^{-3}, as determined by flame emission.

The Raman-region behavior for spectrum II is quite different from that of spectrum I. Saturation measurements for spectrum II are obtained to 300°K, which is sufficiently high that deviations from a two-term polynomial appear. Considering the range below 200°K for a polynomial fit, we find that any value of n greater than 4 is conspicuously unsuitable, and that the preferred form is

$$T_1^{-1}=19T+4.5\times10^{-4}T^{3.6} \text{ sec}^{-1}. \quad (4)$$

The T_1 curve corresponding to (4) is shown with the data in Fig. 7. An exponential function was found not to be suitable as an alternative to the $T^{3.6}$ term.

Each coefficient in (3) and (4) has an experimental uncertainty estimated to be at least 25%. In view of this uncertainty and of the sensitivity of results to impurities and concentration effects in regions where T_1 is large, no significance is attached to the difference in the direct-region coefficients.

The $T^{3.6}$ behavior in the Raman region for spectrum II suggests the situation discussed by Klemens[29] and by Castle *et al.*,[30] where an ion is loosely held in a defect site with a characteristic frequency (and hence a characteristic temperature Θ_i) well below the Debye limit. The result may be an exponential temperature function in the Raman range if the impurity mode is sharp, or a less steep power law (for $T>\Theta_i$) if the vibration is highly damped. A $T^{3.3}$ result for the range 80°–290°K has been reported for Eu^{2+} and for Gd^{3+} in CaF_2.[31]

V. DIELECTRIC RELAXATION

Whereas our EPR spectra are sensitive to ionic arrangements around Mn^{2+} impurities in CaF_2 resulting from exposing the sample to oxygen or to water vapor, the dielectric-loss measurements give information concerning the results of these treatments in the crystal as a whole, with the presence or absence of Mn^{2+} playing a negligible role. Several samples differing in their histories were studied, as follows: (A) Harshaw optical-grade CaF_2; (B) a Harshaw sample subjected to hydrol-

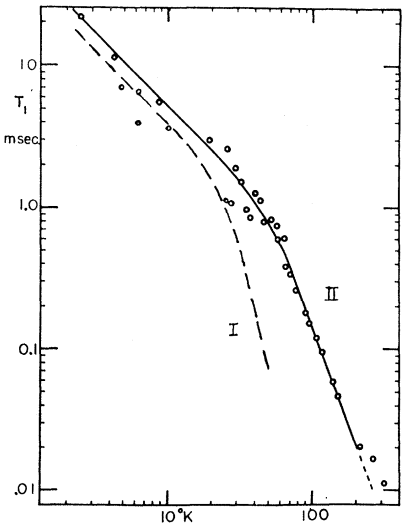

FIG. 7. Measured spin-lattice relaxation time versus temperature for spectrum II. ——Eq. (4); – – – Eq. (3), representing results for spectrum I.

[28] Joseph B. Horak and A. W. Nolle, Phys. Rev. **153**, 372 (1967).

[29] P. G. Klemens, Phys. Rev. **125**, 1795 (1962).

[30] J. G. Castle, Jr., D. W. Feldman, and P. G. Klemens, Phys. Rev. **130**, 577 (1963).

[31] Kazumi Horai, J. Phys. Soc. Japan **19**, 2241 (1964).

ysis at 1000°C in the absence of air for approximately 2 h; (C) a Harshaw sample subjected to oxidation at 1000°C in open air for approximately 2 h; (D) a Harshaw sample held near 700°C for 4 h in air dried in a column packed with anhydrous $CaSO_4$; (E) laboratory-grown $CaF_2:Mn^{2+}$, a sample showing EPR spectrum I; (F) a portion of the preceding sample, subjected to hydrolysis at 1000°C in the absence of air for approximately 2 h.

For samples (A) and (E), which are neither oxidized nor hydrolyzed, a straight-line plot of $\log(\tan\delta)$ versus $\log(f)$ was obtained, where f is the frequency and δ the loss angle. This is attributed to the effect of the conductivity σ, which contributes to $\tan\delta$ the amount $\sigma/\omega\epsilon$, where ϵ is the real part of the dielectric constant. The additional contribution to the loss tangent in the other samples is adequately described, near the respective peaks, by a constant times $2\pi f\tau/[1+(2\pi f\tau)^2]$, a function of the Debye form. Typical loss-tangent data for hydrolyzed samples are shown in Fig. 8 for various

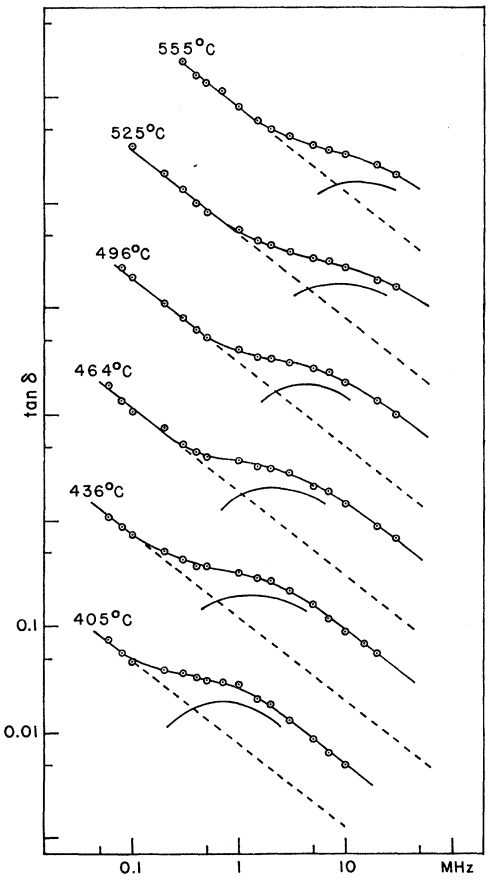

FIG. 8. Dielectric loss tangent versus frequency, at several temperatures, for CaF_2 exposed to water vapor at 1000°C; similar results are obtained with oxygen-treated samples. For clarity, the ordinate is shifted one decade upward for each successive curve.

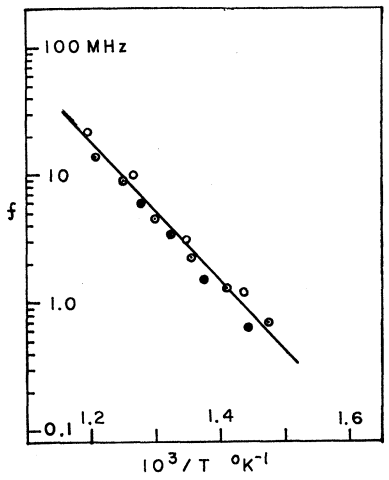

FIG. 9. Activation-energy plot for dielectric loss peaks as in Fig. 8 (composite of data from three samples).

temperatures. A conventional semilogarithmic plot to determine activation energy is shown in Fig. 9, and leads to the expression

$$\tau^{-1}=1.6\times10^{13}\exp(-1.0\text{ eV}/kT)\text{ sec}^{-1}, \quad (5)$$

for the jump rate of the dipoles. The result for oxidized samples is the same.

The relaxation contribution to the loss tangent can easily be made 0.05 to 0.1 (the larger values are more readily obtained by the oxidation procedure). If we suppose that the relaxing polarization is due to an effective dipole moment equal to the F^--to-F^- distance (2.7 Å) times the electronic charge, the concentration required is nearly 0.1 mole%. This large result rules out mechanisms incorporating impurities initially present in the crystal. The small value of the activation energy rules out mechanisms involving thermally produced vacancies. Moreover, the mechanism is one that can be introduced either by oxidation or hydrolysis. We thus conclude that the relaxation process involves the jumping of an O^{2-} impurity ion into a neighboring vacant F^- site which is present for charge compensation.

VI. DISCUSSION

We now offer a provisional explanation of the origin of spectrum II, the cubic spectrum found in samples quenched after being held at high temperatures in the absence of oxygen. The evidence may be summarized as follows: The symmetry of the EPR spectrum, together with the absence of superhyperfine structure, indicates that spectrum II is due to Mn^{2+} ions surrounded by negative ions other than F^-, in an arrangement having cubic, or at least tetrahedral, symmetry, where the symmetry axes coincide with those of the host crystal. The configuration forms at high temperatures (we used 700 to 1050°C) and can be

frozen in by sufficiently rapid cooling. When a sample with the arrangement quenched in is reheated, the spectrum disappears above 380°C. Location of Mn^{2+} in ordinary substitutional sites (spectrum I) is strongly favored by sufficiently slow cooling. Although the spectrum is obtained by the foregoing treatment of "optical-grade" crystals doped with Mn^{2+}, the concentration and rate of formation are greatly increased in the presence of water vapor. Crystals showing spectrum II at intensities corresponding to about 10^{18} ions/cm^3 show weak, sharp infrared-absorption bands apparently identical with those reported[22] following hydrolysis of undoped CaF_2, which have been attributed to local formation of calcium hydroxide.[23]

After considering hydroxyl ions, oxygen ions, and hydrogen negative ions as possible neighbors to the Mn^{2+} ion in spectrum II, we have concluded that the present evidence suggests an environment of eight OH^- ions, replacing the F^- neighbors of the ordinary substitutional site. A strong reason for rejecting the idea of oxygen neighbors is that the only sharp-line spectrum we have obtained by exposing the sample to oxygen is spectrum III. The possibility that the neighbors are H^- was considered when the spectrum was obtained by quenching samples heated in hydrogen. We are not aware of any precedent showing that substitutional H^- can occur in CaF_2, however, and since spectrum II develops still more rapidly in an atmosphere containing water vapor but no neutral hydrogen, we assumed that the effect of the hydrogen treatment is to produce hydroxyl ions by reaction with oxygen already in the crystal; it is well known that oxygen easily contaminates the crystal during growth.[14] Also, the substitution of H^- for F^- as neighbors to the paramagnetic ion would seem to imply that superhyperfine interactions as in spectrum I should again exist, whereas actually spectrum II consists of unstructured lines having widths of about 5 G. No such inconsistency occurs when we postulate OH^- neighbors. The CaF_2 structure would allow each of these to orient as demanded by the electric dipole moment, hydrogen away from the Mn^{2+} ion, leading thus to an EPR linewidth expected to be somewhat smaller than that for the $[Mn(H_2O)_6]^{2-}$ complex; this, under frozen-lattice conditions in a zinc fluosilicate host, is on the order of 10 G.[32,33]

Our value of 6.2×10^{-4} cm^{-1} for the cubic splitting parameter a in spectrum II is ten times the value reported for spectrum I, but we fail to find a corresponding increase in the spin-lattice relaxation rate for spectrum II as compared to spectrum I (here we may refer to the direct-process region, since a difference in temperature dependence complicates the comparison in the Raman region). This suggests that the arrangement of ions proposed to explain spectrum II amounts to a complex more loosely coupled to the crystalline surroundings than the combination of Mn^{2+} surrounded by eight F^- ions. This is consistent with the implications of the temperature dependence of the spin-lattice relaxation rate in the Raman region, discussed in the preceding section.

In order to interpret the observed disappearance of the shfs of spectrum I at 550°C, we note that a line broadening $\Delta\omega\approx2\times10^8$ sec^{-1} would provide the indicated loss of resolution. Self-diffusion of F^- ions with a jump rate $1/\Delta\omega$ could provide this broadening. But Lysiak and Mahendroo,[34] studying the NMR relaxation of F^{19} due to self-diffusion in CaF_2, have found a T_1 minimum, corresponding to a motional correlation time of 0.5×10^{-8} sec, at 850°C; that is, the jump rate that would explain the change in spectrum I at 550°C does not actually occur until 850°C. We therefore suppose that the disappearance of the shfs is controlled by the relaxation time of the Mn^{2+} ion, which therefore must decrease to about 0.5×10^{-8} sec at 550°C.

The disappearance of spectrum II at 380°C is not reversible by slow thermal cycling, and hence is not to be explained in terms of thermally induced broadening mechanisms, but in terms of the loss of the required neighbors to the Mn^{2+} ion. For the time scale of the actual heating experiment, a transition probability of the order of 10^{-2} sec^{-1} or more for diffusional jumping of the neighbors away from the ion would produce an observable decrease of intensity. No simple connection is expected with the elementary processes occurring either in F^- self-diffusion or in our dielectric-loss experiments, since these situations do not involve the special complex of spectrum II. Both of these cases in fact correspond to jump rates at 380°C much greater than required for the gradual destruction of the complex.

The dielectric-loss measurements, by giving similar results for either hydrolyzed or oxidized samples, indicate that O^{2-} concentrations approaching 0.1 mole % are obtained in the bulk of the crystal by either method within a few hours. These times are not long enough to give spectrum II strongly, in the case of oxidation. In this way we dispose of an alternative view which otherwise could be advanced concerning spectrum II, that it is really due to O^{2-} ions, but that hydrolysis rather than direct oxidation is required to produce them within the bulk of the crystal, instead of in disoriented regions of CaO_2 (probably developing at surfaces and cracks), as in spectrum III. This view is not correct, if we accept the interpretation of the dielectric loss in terms of O^{2-} in the bulk of the sample.

The question of whether intermediate OH^- arrangements, such as a set of seven OH^- neighbors and one F^- about the Mn^{2+} ion, are frozen in at concentrations at all comparable to that of spectrum II cannot be answered from our experiments. The total manganese

[32] B. Bleaney and D. Ingram, Proc. Roy. Soc. (London) **A205**, 336 (1951).
[33] B. C. Thompson (private communication).
[34] R. J. Lysiak and P. P. Mahendroo, J. Chem. Phys. **44**, 4025 (1966).

concentration has not been evaluated at successive stages. While no additional EPR spectra which might correspond to the intermediate forms were seen, it is doubtful that these would be sharp enough for detection, in view of the severe axial fields possible at the ion site in the intermediate forms.

It is beyond the scope of this paper to determine in detail the rate constants and free energies for the reactions connecting the two different environments giving spectra I and II. We can only say that the behavior with thermal cycling suggests that II is stable at higher temperatures, including the range 700 to 1050°C, but is metastable at lower temperatures, as shown by its disappearance at 380°K.

Note added in manuscript. Our conclusion that oxidation of $CaF_2:Mn^{2+}$ leads to containment of the manganese ions in disoriented regions of CaO in the crystal is consistent with the following reports on work done with powders: P. H. Kasai, J. Phys. Chem. **66,** 674 (1962); R. L. Hickok, J. A. Parodi, and W. G. Segelken, J. Phys. Chem. **66,** 2715 (1962); J. A. Parodi, J. Electrochem. Soc. **114,** 370 (1967).

PHYSICAL REVIEW VOLUME 163, NUMBER 2 10 NOVEMBER 1967

Overlap Contribution to the Isomer Shift of Iron Compounds*

E. ŠIMÁNEK† AND Z. ŠROUBEK‡
Department of Physics, University of California, Los Angeles, California

(Received 12 June 1967)

The electron density $\Psi^2(0)$ at the iron nucleus in oxides is calculated as a function of the Fe–O distance, by taking into account the overlap of the inner shells of iron with the oxygen $2p$ wave functions. The calculation shows the importance of the intershell terms, which effectively reduce the overlap-induced electron density. By comparing these results with the high-pressure isomer-shift measurements of divalent iron in CoO, the relative change of the ^{57}Fe nuclear radius is found to be less than -4.0×10^{-4}. The overlap effect provides an important amplification mechanism for the contribution of $4s$ bonding to $\Psi^2(0)$. On the basis of this mechanism, large increases in $\Psi^2(0)$ observed on going from Fe^{2+} to Fe^{3+} salts can be explained by a reasonable increase in the amount of $4s$ bonding.

I. INTRODUCTION

IT is well known that the Mössbauer isomer shift (I.S.) depends primarily on the difference in the electron charge density at the nucleus between the absorber and emitter. In the nonrelativistic approximation, this dependence can be written as follows[1]:

$$\text{I.S.}=\tfrac{2}{5}\pi Ze^2(R_{\text{exc}}^2-R_{\text{gd}}^2)[\Psi_A^2(0)-\Psi_E^2(0)], \quad (1)$$

where R_{exc} and R_{gd} are the nuclear-charge radii of the first excited and ground states, and $\Psi_A^2(0)$ and $\Psi_E^2(0)$ are the s-electron densities at the nucleus for the absorber and emitter, respectively. Equation (1) has been used by Walker *et al.*[1] to calibrate the isomer shift of ^{57}Fe. Their procedure was based on the observation that the isomer-shift difference between various ionic ferrous and ferric absorbers, relative to a common source, has a constant value of about 0.9 mm/sec. By assuming that $\Psi^2(0)$ in these salts is correctly given by the computations of Watson[2] for $3d^5$ and $3d^6$ free ions, Walker *et al.*[1] determined the relative change of the nuclear charge radius to be

$$\Delta R/R=(R_{\text{exc}}-R_{\text{gd}})/R_{\text{gd}}=-1.8\times10^{-3}. \quad (2)$$

Watson's[2] results predict a change in $\Psi^2(0)$ from 118.813×10^2 to 118.796×10^2 a_0^{-3} on going from Fe^{3+} to Fe^{2+}. The small difference between the latter values ($=1.76$ a_0^{-3}) is almost entirely due to the shielding of the $3s$ wave function by the additional $3d$ electron. The contribution of the $3s$ wave function to $\Psi^2(0)$ is 140 a_0^{-3}, and it is obvious that a small deviation from this Hartree-Fock value, due to correlation, could lead to a considerable uncertainty in the calibration of the ^{57}Fe isomer shift. Another source of error comes from the effect of the $3d$ and $4s$ covalent bonding, which is very difficult to estimate with sufficient accuracy. It is interesting to note that smaller values of $\Delta R/R$ have been predicted by Goldanskii[3] and Danon[4] on the basis

* Supported in part by the National Science Foundation and the Office of Naval Research, Grant No. NONR 233(88).

† On leave from the Institute of Physics, Czechoslovak Academy of Sciences, Prague, Czechoslovakia.

‡ On leave from the Institute of Radio Engineering and Electronics, Czechoslovak Academy of Science, Prague, Czechoslovakia.

[1] L. R. Walker, G. K. Wertheim, and V. Jaccarino, Phys. Rev. Letters **6,** 98 (1961).

[2] R. E. Watson, Solid State and Molecular Theory Group, Technical Report No. 12, Massachusetts Institute of Technology, 1959 (unpublished).

[3] V. I. Goldanskii, in *Proceedings of the Dubna Conference on the Mössbauer Effect* (Translated by Consultants Bureau Enterprises, Inc., New York, New York, 1963), pp. 17–19.

[4] J. Danon, in *Applications of the Mössbauer Effect* (International Atomic Energy Agency, Vienna, Austria, 1966), Series No. 50, p. 89.